This article was downloaded by: *[Kordesch, Martin]*
On: *6 January 2009*
Access details: *Access Details: [subscription number 907395992]*
Publisher *Taylor & Francis*
Informa Ltd Registered in England and Wales Registered Number: 1072954 Registered office: Mortimer House, 37-41 Mortimer Street, London W1T 3JH, UK

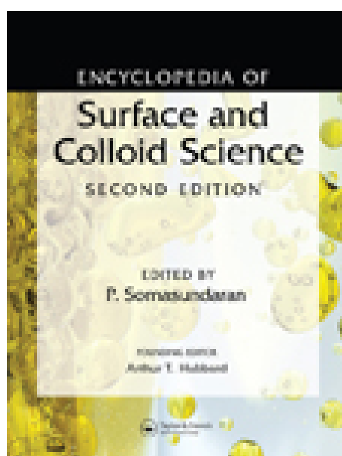

Encyclopedia of Surface and Colloid Science
Publication details, including instructions for authors and subscription information:
http://www.informaworld.com/smpp/title~content=t713172975

Synchrotron Radiation Photoemission Electron Microscopy

Martin E. Kordesch [a]; Stefan Heun [b]
[a] Department of Physics, Ohio University, Athens, Ohio, U.S.A. [b] NEST CNR-INFM and Scuola Normale Superiore, Pisa, Italy

Online Publication Date: 17 November 2008

To cite this Section Kordesch, Martin E. and Heun, Stefan(2008)'Synchrotron Radiation Photoemission Electron Microscopy',Encyclopedia of Surface and Colloid Science,1:1,1 — 16

PLEASE SCROLL DOWN FOR ARTICLE

Full terms and conditions of use: http://www.informaworld.com/terms-and-conditions-of-access.pdf

This article may be used for research, teaching and private study purposes. Any substantial or systematic reproduction, re-distribution, re-selling, loan or sub-licensing, systematic supply or distribution in any form to anyone is expressly forbidden.

The publisher does not give any warranty express or implied or make any representation that the contents will be complete or accurate or up to date. The accuracy of any instructions, formulae and drug doses should be independently verified with primary sources. The publisher shall not be liable for any loss, actions, claims, proceedings, demand or costs or damages whatsoever or howsoever caused arising directly or indirectly in connection with or arising out of the use of this material.

Synchrotron Radiation Photoemission Electron Microscopy

Martin E. Kordesch
Department of Physics, Ohio University, Athens, Ohio, U.S.A.

Stefan Heun
NEST CNR-INFM and Scuola Normale Superiore, Pisa, Italy

Abstract
Synchrotron radiation photoemission electron microscopy is an imaging method that uses synchrotron radiation to produce photoelectrons that are collected and used to image a surface. The method has many variations, other names, but is abbreviated here as "SR-PEEM" for simplicity.

Downloaded By: [Kordesch, Martin] At: 00:51 6 January 2009

INTRODUCTION

Synchrotron radiation photoemission electron microscopy is an imaging method that uses synchrotron radiation to produce photoelectrons that are collected and used to image a surface. The method has many variations, other names, but is abbreviated here as "SR-PEEM" for simplicity.

Visible light microscopy is the earliest form of microscopy. It revolutionized the understanding of the small-scale physical world. In the 20th century, electron microscopy became a universal tool in science and medicine. In this century, the advances in synchrotron radiation sources around the world enable the use of "light" microscopes operating at wavelengths in the vacuum ultraviolet, soft X-ray, and hard X-ray regions of the spectrum. Synchrotron radiation offers high brightness and, most importantly, the ability to vary or scan the incident light wavelength. As with visible light microscopy, the frontier of this branch of science is equally divided between improvements in methodology and instrumentation, and the applications of the method to specific problems.

SYNCHROTRON RADIATION BASED MICROSCOPY

Synchrotron radiation is produced when relativistic electrons (or positrons) are accelerated along a curved path by the so-called bending magnets. This change in their direction is an acceleration, and an accelerated charge emits electromagnetic radiation. Synchrotron radiation is usually associated with the narrow, collimated beam of light that is radiated along the forward tangent of the orbit by relativistic electrons. The charged particles follow a curved path on the order of meters, and the beam is radiated tangentially to the plane of their orbit. The light has a large spectral range, and is polarized. A recent review is contained in Ref.[1].

In modern synchrotron light sources, the brightness of the radiation is increased by orders of magnitude using so-called "insertion devices" (undulators and wigglers).[1,2] These devices are inserted into the drift (straight) portions of the storage ring and generate radiation as highly relativistic electrons traverse a periodic magnetic field structure. Undulators use weak magnetic fields resulting in gentle periodic excursions of the electrons. In this way, the light cones just overlap and interfere with each other, so that certain wavelengths of light are enhanced, i.e. the natural bandwidth of the central emission cone is reduced, while at the same time the characteristic X-ray emission angle becomes narrower when compared with the natural emission angle of a bending magnet. The emission wavelength can be changed by altering the gap between the component magnets so that the light is tunable to specific wavelengths. On the other hand, wigglers use high magnetic fields; therefore, the electron acceleration is stronger, resulting in a broad emission spectrum similar to a bending magnet, but with enhanced photon flux and energy width. Details of modern synchrotron light sources can be found on the worldwide web at http://lightsources.org.

There are many reasons why synchrotron radiation is attractive for microscopy. For simple magnification, electron and scanning probe microscopes are already far ahead of any synchrotron-based method. In terms of contrast, however, there are advantages to synchrotron radiation. Atomic transitions, specific to each element, from valence and core levels, are within the spectral range of synchrotron radiation. Element-specific imaging is possible, with spectroscopic resolution, in addition to imaging.

Two general types of microscopes are used for photoemission microscopy. One type (SR-PEEM)

Encyclopedia of Surface and Colloid Science DOI: 10.1081/E-ESCS-120040641
Copyright © 2008 by Taylor & Francis. All rights reserved.

uses a direct imaging electron optical system, i.e. the image is not composed of scanned lines. Here, the surface is illuminated over the entire field of view, and the photoelectrons are collected all at once. This approach is sometimes called spectro-microscopy. The second type, scanning photoemission microscopy (SPEM), uses a small focused spot that is scanned over the surface, and an image is composed of an array representing the emitted photoelectron yield at each point. This approach can be classified as micro-spectroscopy.[1]

Photoemission electron microscopy (PEEM) is described in another article.[3] The principles underlying the basic function of the electron optical side of the microscope are very similar in SR-PEEM and PEEM. When photons are incident on a surface, electrons can be emitted, and collected by the electron optical system. The origin of these photoelectrons depends on the incident photon energy. Laboratory PEEM instruments use a light source with a fixed spectrum. A mercury arc lamp is typical. As much of the emitted electron distribution as possible is collected by the objective. A ''white light'' image, i.e., using the synchrotron beam without monochromator or the ''zero-order'' reflection would give operating conditions that are, in principle, similar to a laboratory PEEM (but with much different results, owing to the larger incident spectral width).

In SR-PEEM, there are two different methods for utilizing the variable wavelength of SR light. One of these is based on total yield measurements.[4] In this version of SR-PEEM, the incident wavelength is varied, and all photoelectrons are collected, without energy-discrimination. An example would be images acquired above and below an absorption edge for a specific element. The difference in the contrast in the images gives information on the distribution of that element. Because the image acquired above the absorption edge includes electrons that are not present in the below-edge image, image contrast due to that element is present. The absorption edge spectrum is obtained by recording the image intensity as a function of photon energy (micro X-ray absorption near edge spectroscopy (μ-XANES)).

A second method, partial yield detection, is also possible with some SR-PEEM systems. In this method, the electrons are analyzed using an imaging electron spectrometer to determine the energy distribution of, or select a portion of, the photoelectrons collected by the imaging optics. The electron spectrometer is usually located after the objective lens, but before the imaging device that converts the electron yield to a visible image. Image contrast can be obtained at a fixed photon energy or by selecting an electron energy window for analysis and varying the incident photon energy. By selecting only a fraction of the emitted photoelectrons, image intensity becomes a concern. One of the advantages of modern synchrotron light sources is their high brightness, which makes partial yield detection practical.

The basic fact that synchrotron light can be tuned over a large energy range (from the UV to X-rays) extends the chemical contrast available in SR-PEEM relative to PEEM. The incident photon energy can be varied, the photoemitted electrons can be energy-analyzed and polarization effects can be used in some cases to analyze molecule-surface orientations. The variable incident photon energy lets the user choose the optimum contrast for a particular element. If the sample is robust enough for longer-term measurements, the user can tune the incident light for optimal contrast for several different elements.

Modern digital imaging techniques allow storage of a large number of high-resolution images. Each image, collected at a different incident photon energy, is a pixel-by-pixel map of the electron yield. When a number of sequential images are acquired, the electron yield–photon energy curve at each pixel is measured. Sometimes, this is called a ''stack'' of images (see, for example, Ref.[5]). The ''stack'' is an electron spectrum at each location in the image. The analysis of the ''stack'' can then be used to generate images that show contrast correlated with a specific element, or any other resolvable spectral feature. In addition, if the total electron yield is analyzed in some way, say by filtering, or selection of a particular energy range, the contrast can be further enhanced by measuring the partial electron yield at each pixel.

Both direct imaging and scanning X-ray microscopes can make use of this type of image analysis. In the direct image, the intensity is measured for all of the pixels at one energy, for the scanning microscopes, the electron yield is analyzed over several energy ranges one pixel at a time.

PHOTOEMISSION MICROSCOPY: PAST, PRESENT, AND FUTURE

Early application of SR light to photoemission microscopy was by two techniques that are no longer popular. The first is to use the soft X-rays to induce fluorescence and then to convert the fluorescence X-rays to photoelectrons, which are imaged using electron optics or an electron-to-visible light converter.

[1]Very recently also a third method has been demonstrated with sub-100 nm lateral resolution: the so-called lensless imaging which uses the measured diffuse x-ray intensity from the sample to reconstruct an image of the sample. For details, see S. Eisebitt et al., Nature **432** (2004) 885.

Downloaded By: [Kordesch, Martin] At: 00:51 6 January 2009

This technique used transmission geometry, with the object located on or near the photocathode; it is reminiscent of ''contact printing'' as used in photography.[6] The second early form used a strong divergent magnetic field to project the emitted photoelectrons onto an imaging screen: magnetic projection photoelectron microscopy.[7,8] The second method is the ancestor of the spectro-microscopy technique, even though the resolution and magnification were limited, because it involved non-contact formation of an image using emitted photoelectrons during variation of the incident photon energy. Currently, most SR-PEEM instruments use a high electric field and electrostatic or magnetic lenses for imaging. An early version was developed by Tonner and Harp.[4] SPEMs were developed concurrently.[9]

Advances in SR-PEEM have been a result of advances in the synchrotron sources and focusing methods for X-rays. In very recent times, the improvement of electron optical methods for aberration correction and energy filtering has played an increasingly important role.

Modern instruments vary widely in complexity and application. Some have complicated acronyms that describe what they can do, up to and including SMART: ''spectromicroscope for all relevant techniques''.[10]

The history of PEEM can be read in many places; see Griffith and Engel[11] for a review of progress up to ultrahigh vacuum microscopes, and more recently Guenther et al. (2002).[12] Reviews of instrument parameters for the many modes of operation and the considerations for instrument design can be found in Rempfer and Griffith[13] and Veneklasen.[14] The conference series on the vacuum ultraviolet ''VUV'', for example, is also a good source of recent advances.

Possibly, the fastest growing area of SR-PEEM is imaging magnetic materials (see Ref.[15]). The development of picosecond imaging has enabled the observation of dynamic magnetic processes in materials. The application of SR-PEEM is also growing to include soft materials, minerals, biological samples, and technologically important materials such as semiconductors and nanomaterials, and tribology.

PHOTOEMISSION MICROSCOPY: INSTRUMENTATION

General Remarks

Before we discuss in detail the various photoemission electron microscopes operating at synchrotron light sources, we will first consider some general aspects of microscopy using X-rays. Given by the detection scheme, two groups can be identified: (a) photon in–photon out, and (b) photon in–electron out. In (a), we have the X-ray transmission microscopes and the fluorescence microscopes.[16] Owing to the large X-ray attenuation length of a solid, these microscopes are rather bulk-sensitive (100 nm sampling depth and more).[17] Work in transmission requires thinned samples (thickness around 100 nm).[18] On the other hand, the detection of photoelectrons results in very surface sensitive measurements, because the escape depth of the photo-excited electrons in the energy range of interest here is a few Angstrom to a few nanometers only.

Scanning Photoemission Microscopy (SPEM)

In a scanning microscope, the light is focused by an optical element (usually a Fresnel zone plate or a Schwarzschild objective) on a small spot (diameter around 100 nm) on the sample.[19] A high brightness source is needed. Since the lateral resolution of these microscopes is obtained by focusing the light in a small spot, their ultimate resolution is diffraction-limited. The excited photoelectrons are collected by an electron energy analyzer with a typical energy resolution of 200 meV or better.[19] This is sufficient for the detection of chemical shifts in core level peaks[20] and for valence band spectroscopy.[21] Samples do not need to be flat, so that, for example, measurements on cross-sectioned samples can be performed.[22] Drawbacks of this design are the poor time resolution caused by the need to scan the sample relative to the light spot, and the high photon flux in a small spot, which might locally charge or damage the sample.[23]

A typical setup for a scanning photoelectron microscope (SPEM) employing a Fresnel zone plate is the ESCA microscope at the Elettra synchrotron radiation source in Trieste, Italy.[24] A sketch of this beamline is shown in Fig. 1. Fresnel zone plates are circular diffraction gratings made of an alternating sequence of absorbing and transparent rings. In certain distances from the zone plate, all transmitted lightwaves will have a phase difference of $2\pi n$ (n integer), i.e. the condition of constructive interference is met. Therefore, zone plates act as lenses with several foci. To block the higher order foci, an order-selecting aperture (OSA) is used. The (unfocused) zero-order light is blocked by a central stop in the zone plate. The efficiency of modern zone plates can reach 55% for hard X-rays (7 keV). For soft X-rays ($h\nu < 1$ keV), an efficiency of 10% is routinely achieved. The minimum spot size that can be obtained is 1.22 times the width of the outermost ring.[25] Nanolithography is therefore required to produce zone plates with nanometer spot size. A typical focal length of a zone plate lens for light with 500 eV is several millimeters. Since

Downloaded By: [Kordesch, Martin] At: 00:51 6 January 2009

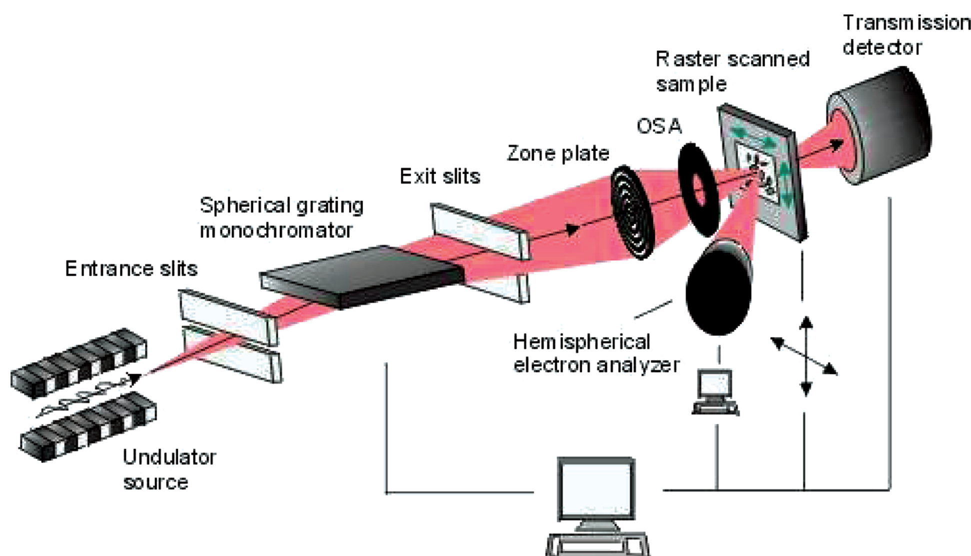

Fig. 1 Schematic drawing of the ESCA microscopy beamline at Elettra hosting an SPEM with Fresnel zone plate and order sorting aperture (OSA) as focusing system. *Source*: From http://www.elettra.trieste.it/experiments/beamlines/esca/index.html.

Downloaded By: [Kordesch, Martin] At: 00:51 6 January 2009

the focal length is proportional to the photon energy, imaging at much lower photon energies would result in unpractical small working distances. Therefore, zone plates are not used in photoemission at photon energies below 300 eV.

A typical setup for an SPEM station employing a Schwarzschild objective is the Spectromicroscopy beamline at the Elettra synchrotron radiation source in Trieste, Italy.[26] A sketch of this beamline is shown in Fig. 2. A Schwarzschild objective consists of a concave and a convex mirror. The radiation impinges nearly orthogonal on the mirror surfaces. Since the reflectivity of metals for normal incidence in the VUV and for X-rays is very small (<1%[17]), multilayer coatings have to be employed. They enhance the reflectivity by constructive interference of the wavefronts reflected at the single layer boundaries. This condition is met if the wavelength equals two times the layer thickness. Modern multilayer coatings can reach, in a small energy range, reflectance values of the order of 50%.[27] This implies that a dedicated Schwarzschild objective is needed for each photon energy so that scans of photon energy are practically impossible.[27] Since each layer of the coating has a thickness

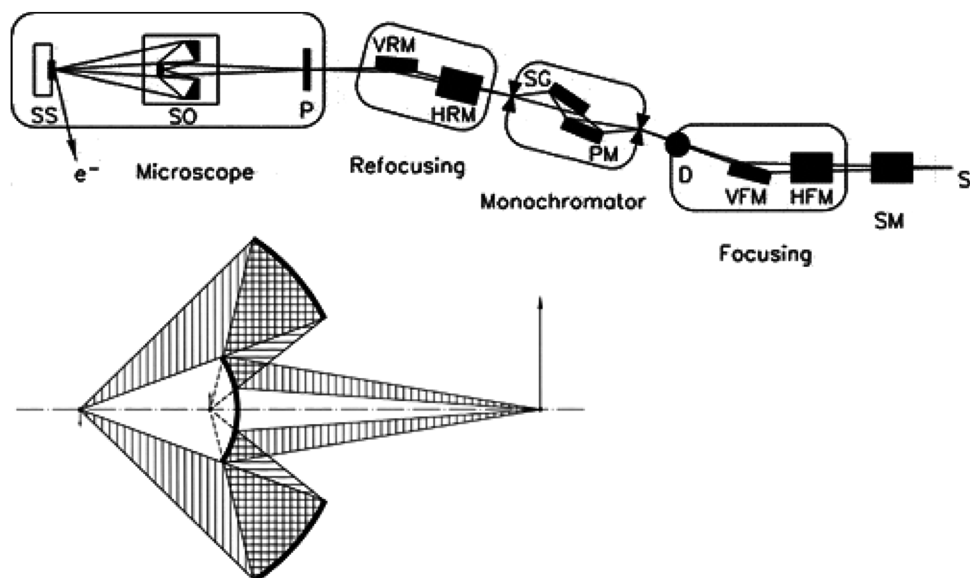

Fig. 2 Sketch of the Spectromicroscopy Beamline at Elettra, Trieste, Italy, which uses Schwarzschild objectives (SO). The inset shows the X-ray traces within the objective. *Source*: From http://www.elettra.trieste.it/experiments/beamlines/spectro/index.html.

comparable with the photon wavelength, surface, and interface roughness prevents the use of Schwarzschild objectives for shorter wavelengths, i.e. higher energies ($E > 300$ eV).[28] In summary, the use of Fresnel zone plates for photoelectron spectroscopy at photon energies below about 300 eV is unpractical owing to their short focal length, and exactly in this low energy range, the Schwarzschild objectives show their best performance.

Photoemission Electron Microscopes (PEEM)

Among the various imaging photoelectron microscopes by far, the most popular today is the photoemission electron microscope (PEEM). In this setup, the light is homogeneously illuminating a spot of several micrometers diameter on the sample. This spot size is still small relative to what is used in classical (integral) setups, but it is large when compared with what is required in the scanning type design, so that illumination can still be achieved with conventional optical elements (mirrors). A PEEM employs electrostatic or magnetic lenses to form a magnified image of the sample on a screen. No sample scanning is necessary. Typical fields of view of the microscope range from 1 μm to 100 μm. Continuous imaging at video rates are possible.[29] A basic PEEM is shown in Fig. 3. The photoelectrons emitted from the sample are accelerated by a high electric field between the sample and the objective lens. The image produced by the objective lens is

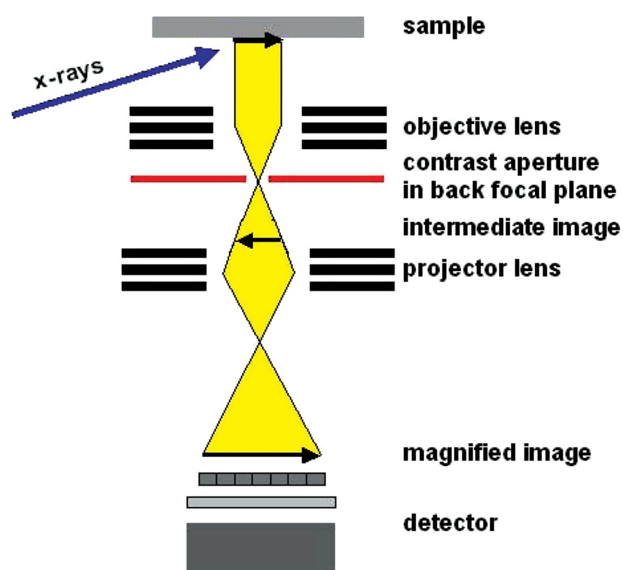

Fig. 3 A schematic drawing of a PEEM. The sample is illuminated by monochromatic X-rays. The lateral photoelectron distribution is obtained by a detector consisting of a multichannel plate, a phosphor screen, and a CCD camera.

magnified by the projector lens(es) onto a detector. Such PEEM systems can reach a lateral resolution of up to 20 nm.[30–34] In brief, the PEEM is a simple instrument with good time resolution. No complicated X-ray optics is needed, no sample scanning necessary.

Early PEEM work was performed with deuterium or mercury lamps.[4,29] For element-specific imaging, higher photon energies are necessary to excite atomic core levels. Therefore, spectroscopic imaging with PEEM is usually done at a synchrotron. Most of this work has utilized soft X-rays and ultraviolet photons (10–2000 eV) to achieve high surface sensitivity. However, there are first attempts to use PEEM in combination with hard X-rays, which would make PEEM a bulk sensitive probe.[35]

One way to perform spectroscopy with a PEEM is to scan the photon energy and to perform optical absorption edge spectroscopy with the lateral resolution of the PEEM (μ-XANES). It is possible because the total photoelectron yield is almost proportional to the photoabsorption coefficient.[36] This technique is very useful for the study of organic and magnetic materials.[37] A requirement for this kind of experiments is a tunable X-ray source, which is naturally given in a synchrotron.

Even with sufficiently high photon energies, a standard PEEM cannot be used for micro X-ray photoelectron spectroscopy (μ-XPS) because it is not equipped with a photoelectron energy analyzer. The implementation of an energy filter in a PEEM is, however, not only useful to obtain energy filtered images and to collect photoemission spectra. The lateral resolution of this instrument is not limited by diffraction, but rather by lens aberrations. Therefore, the spatial resolution of a PEEM can be increased by reducing the aberrations. One way to do this is to add an energy filter to the PEEM.[32,38,39] This reduces chromatic aberrations. Therefore, even for μ-XANES experiments, the use of an energy analyzer is beneficial: it allows the selection of a narrow energy window around the maximum of the secondary electron energy distribution and thus improves the lateral resolution without an unacceptable loss of image intensity.

Two principal ways lead to an energy analysis of the photoelectrons with lateral resolution. One possibility is to use an aperture and to select an interesting region within the field of view. Photoelectrons from other parts of the sample are blocked, and only the photoelectrons from the interesting region can reach the analyzer. Therefore, the PEEM acts as a high-performance transfer lens for the analyzer. The diameter of the analyzed region can be as small as 1 μm. A commercial energy analyzer can be used for this purpose, which allows the use of well-tested standard equipment.[30,40]

The second possibility is to energy-filter the entire PEEM image. Several methods have been proposed

Downloaded By: [Kordesch, Martin] At: 00:51 6 January 2009

to achieve this goal. In a simple setup, a retarding field analyzer can be used. A mesh or grid is inserted in the PEEM optics after the magnification stages, but before the image detector. If the mesh is biased, only photoelectrons with a kinetic energy higher than the bias can pass the mesh, which therefore acts as a high-pass filter. By increasing the bias of the mesh, more and more photoelectrons are cut out, and the energy spread in the image is reduced. By differentiation, the energy distribution curve of the photoelectrons from the sample can be obtained. An energy resolution of better than 1 eV is reported for this setup with synchrotron and laboratory X-ray sources.[41]

In a more sophisticated setup, the whole PEEM image is energy filtered by a band-pass filter, i.e. only electrons with a certain energy $E_0 \pm \Delta E$ can contribute to the image. Different solutions have been proposed to realize such a band-pass filter:

1. A time-of-flight tube in the PEEM. This requires a pulsed light source. A first demonstration of this setup has been given at BESSY operated in single bunch mode.[42–44]
2. A Wien filter uses an electric and magnetic field, which are perpendicular to each other so that only electrons with a particular energy can pass the filter without deflection.[38,39,45] Although an energy resolution of 0.1 eV has been calculated for this design, only 1 eV has been demonstrated so far, mainly because at higher resolution, the intensity would be unacceptably low.[46]
3. An electrostatic spherical energy analyzer, like in a conventional XPS setup.[47,48] Results have been obtained with spherical 90° and 180° systems.[49–51] A combination of two 90° analyzers has been proposed.[52]
4. An Omega filter. This imaging energy filter consists of four sector magnets arranged like the Greek capital letter omega. It will be used in the SMART microscope.[10] A maximum energy resolution of 0.1 eV has been calculated.[53]

Most of the results in photoelectron spectroscopy using a PEEM published so far have been obtained with electrostatic hemispherical analyzers. In any case, in contrast to conventional spectroscopy, an imaging energy analyzer used in a PEEM has not only to provide high energy resolution, but it should also provide an image free of distortions.

A lateral resolution of 22 nm and an energy resolution of better than 0.2 eV have been achieved with the spectroscopic photoelectron and low energy electron microscope (SPELEEM), which is based on a design by Veneklasen and Bauer.[14,49] A schematic drawing of it is shown in Fig. 4. Besides being a PEEM, this microscope is also equipped with an electron gun to perform low energy electron microscopy (LEEM) with a lateral resolution of 8 nm.[54] The separation between incoming and outgoing electrons is achieved by a magnetic prism (sector field). The electrons emitted or reflected from the surface are transferred into the

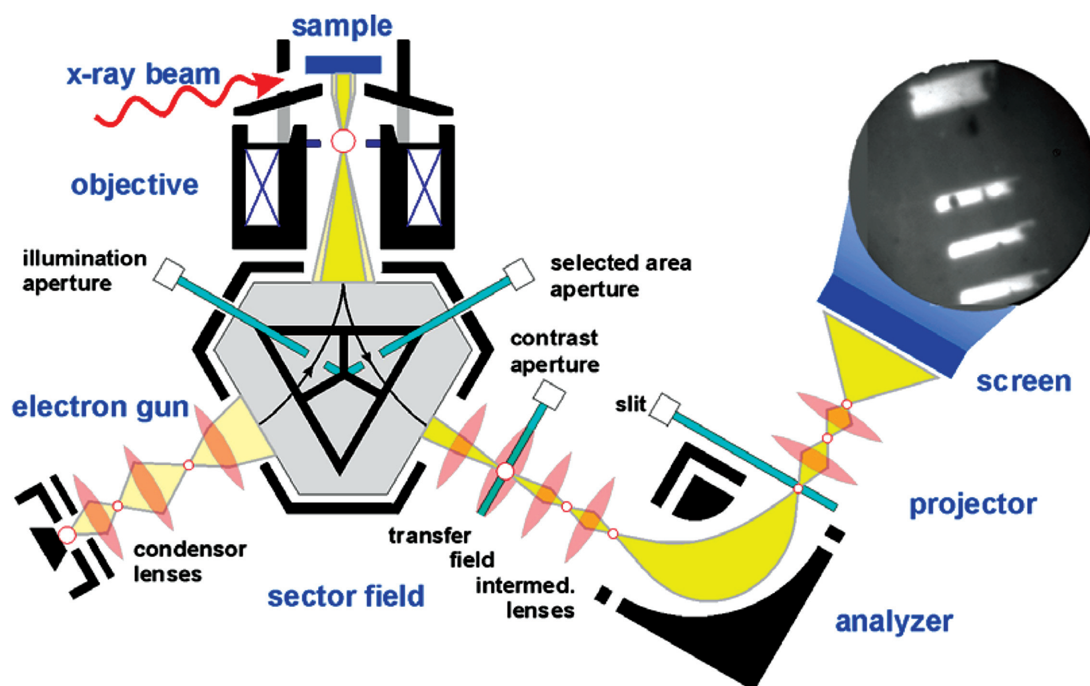

Fig. 4 Schematic drawing of the SPELEEM instrument.

Downloaded By: [Kordesch, Martin] At: 00:51 6 January 2009

image plane of the microscope, where a magnified image of the sample can be observed with a video camera or a slow scan CCD camera. When used as an electron microscope, the SPELEEM can be used to obtain real space images of the sample (LEEM) or to measure the intensity distribution in reciprocal space (low energy electron diffraction (LEED)). Furthermore, the use of the energy analyzer allows measurement of the energy distribution of the electrons (electron energy loss spectroscopy (EELS)). Both LEED and EELS can be measured from a micrometer spot on the sample. In complete analogy to this, three modes of operation are available when working with photons: PEEM as well as photoelectron diffraction (PED) and photoelectron spectroscopy (PES). Details on the use of this instrument can be found in Refs.[32,51].

A new generation of PEEMs is under construction in different laboratories: the SMART project at BESSY,[10] the PEEM-III project at the ALS,[55] and the XPLEEM project from Delong Instruments.[56] These instruments will be similar to the SPELEEM, but they will use an electron mirror in the electron-optical path for aberration correction.[57] Their lateral resolution is calculated to be a few nanometers.[58]

APPLICATIONS AND EXAMPLES

Magnetism

In the last decade, PEEM has become a very popular technique to visualize magnetic domains at surfaces. For a review, see Ref.[15]. In combination with circularly polarized light, the X-ray magnetic circular dichroism (XMCD) effect can be employed as a contrast mechanism for magnetic domain imaging.[59,60] XMCD image contrast arises from the dependence of the photoabsorption coefficient on the relative orientation of the sample magnetization direction with respect to the helicity of the incident X-rays: it is maximal for parallel alignment, minimum for antiparallel alignment, and zero for perpendicular alignment. Since electrons are excited from core levels to empty states, XMCD is element-specific. This is very useful especially for the study of magnetic multilayers and alloys. Furthermore, the XMCD measurements can be quantitatively evaluated via sum rules to obtain the spin and orbital magnetic moments and their anisotropies.[61] Fig. 5 shows images obtained from a Co film deposited on a patterned Si substrate (four squares of size 1 μm and height 110 nm). The Co was deposited under grazing incidence, which leads to the formation of shadow regions above the squares, which are without Co. The images in Fig. 5(A) and (B) are SR-PEEM images taken at the Co L_3 edge with negative and positive helicity, respectively. The sample was oriented in a

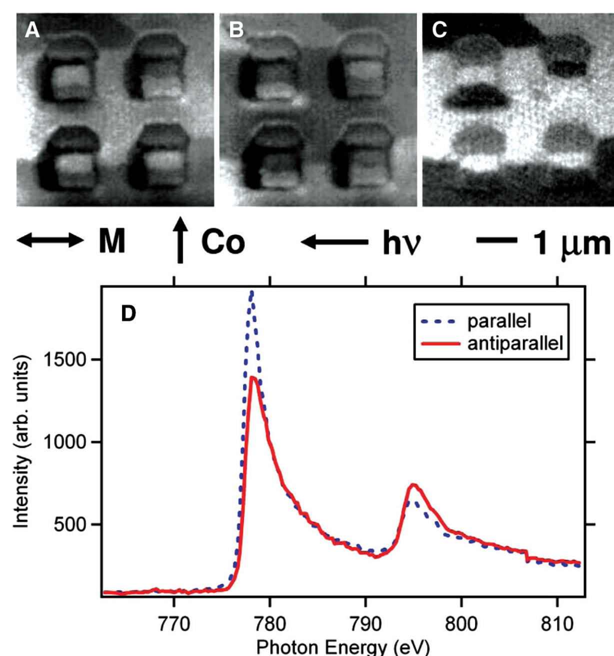

Fig. 5 XMCD-PEEM images of a Co film deposited on a patterned Si substrate, measured at the Co L_3 edge. (A) and (B) show images taken with negative and positive helicity, respectively; (C) is the difference between the two images. (D) Co L_{23} edge absorption spectra measured on the same sample with photons of positive helicity. The spectrum indicated by the dashed line was measured on an area where the magnetization was parallel to the helicity vector of the X-rays, while the spectrum indicated by the full line was measured in an area with antiparallel magnetization.

way that the magnetization in the film was (anti) parallel to the incoming light, which was illuminating the sample under grazing incidence (16° from the right). Fig. 5(C) shows the difference between the two images in (A) and (B). Although the magnetic domain contrast can already be detected in the raw data, it is greatly enhanced in the difference image: in the bright areas the sample magnetization is parallel to the helicity vector of the X-rays, in the dark areas antiparallel. While the shadow of the light (to the left of the squares) is visible in the raw data as region of lower intensity (the light is not completely attenuated by the Si squares), this effect cancels out in the difference image. On the other hand, the regions without Co are clearly visible in the difference image as non-magnetic (i.e. gray) regions. Fig. 5(D) shows Co L_{23} edge absorption spectra, which were measured on the same sample with photons of positive helicity. The spectrum indicated by the dashed line was measured on a flat area away from the pattern where the magnetization was parallel to the helicity vector of the X-rays (equivalent to a bright area in Fig. 5(B)), while the spectrum indicated by the full line was measured in a dark area. The intensity difference in the spectra at the Co L_3 edge

Downloaded By: [Kordesch, Martin] At: 00:51 6 January 2009

explains the contrast observed in the image shown in Fig. 5(B). At the Co L_2 edge, the spectral intensity is inverted, which also reflects in a contrast inversion in the SR-PEEM image (not shown here). Inverting the helicity of the X-rays, the two spectra show an inverted behavior (not shown here), which reflects in the contrast inversion observed between the images in Figs. 5(A) and (B).

In a similar fashion as XMCD, also the X-ray magnetic linear dichroism can be employed for the study of antiferromagnetic thin films.[37,62] Finally, in yet another approach, the magnetic sensitivity is obtained by measurement of the spin-polarization of the emitted photoelectrons.[63]

Very recently, attention has focused on time-resolved studies of magnetization dynamics with PEEM. As already mentioned, PEEM allows continuous imaging with video rate. The temporal resolution of PEEM can, however, be dramatically enhanced by a pump and probe approach with two pulsed excitation sources, which are synchronized for stroboscopic imaging. Using a laser for pumping (the width of the laser pulse can easily be less than 1 ps, down to some fs), the X-ray pulses from a synchrotron can be used for probing. In a third-generation synchrotron, the X-ray pulses have a typical width of 50–100 ps. In multibunch operation of the light source, they are repeated every few ns, which is too short for most time-resolved experiments, given the X-ray pulse width. However, when the synchrotron is operated in single bunch mode, the time interval between X-ray pulses is around 1 μs, which is sufficiently long when compared with the X-ray pulse width. A hybrid mode has been proposed at the Swiss Light Source, in which a single pulse is located in the regular 180 ns gap in the filling pattern in multi-bunch mode. During measurements, all but the single pulse are blanked out by a gated detector in the PEEM, which has a rise time of 20 ns.[64,65]

The principle of these experiments is sketched in Fig. 6. The pump pulse excites the sample, and after a constant delay Δt the X-ray pulse from the synchrotron probes the sample. Averaging over many pulses allows the collection of images with a useful signal—to-noise ratio. This method can be applied only to systems that return to their initial state between two probe pulses. By changing Δt, the temporal evolution of the sample can be obtained with a time-resolution given by the X-ray pulse width. Pulse length of some ten fs are expected for X-ray free electron lasers (XFEL), which are now under construction in several places worldwide. Using the combination of a Ti:sapphire laser and a PEEM, the surface plasmon dynamics in nanoscale roughness on a silver grating has already been investigated with sub-fs temporal resolution.[66] Furthermore, XFEL sources will deliver such a high photon flux that single shot measurements will become feasible, which would allow to achieve fs-time resolution even with samples that show non-periodic behavior.

Recently, the pump and probe technique has been used in combination with XMCD–PEEM to obtain the response of a magnetic pattern to a short (≈ns) external magnetic field pulse, which has been

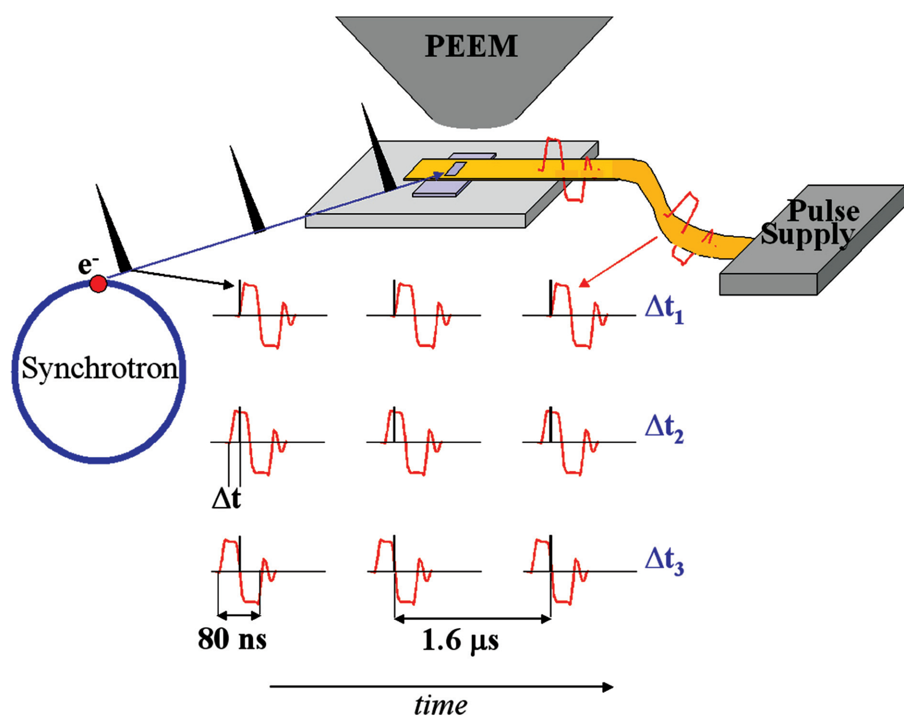

Fig. 6 The principle of a pump and probe experiment with a PEEM microscope. A (magnetic) pump pulse is periodically applied to the sample. These pulses are synchronized with the X-ray pulses from the synchrotron, which probe the sample. Images are taken for several time delays Δt between pump and probe pulses. Image courtesy of Jan Vogel.

Downloaded By: [Kordesch, Martin] At: 00:51 6 January 2009

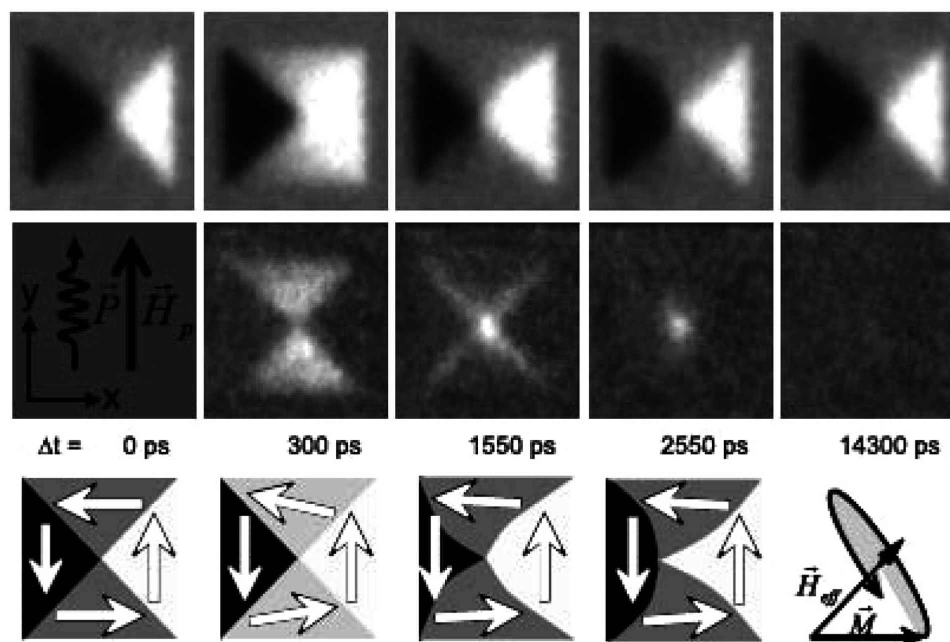

Fig. 7 XMCD images showing the time evolution of a Landau flux-closure pattern in a permalloy square in response to a short in-plane magnetic pulse. *Source*: from Refs.[64,65].

synchronized to the X-ray pulses. The vortex dynamics of Landau patterns has been measured with sub-ns-resolution.[66–69] As an example, Fig. 7 shows in the first row the time evolution of a Landau flux-closure pattern in a permalloy square in response to a short in-plane magnetic pulse.[64,65] The sketch in the second row shows the direction of the applied magnetic field **H** and the X-ray polarization vector **P**. The images in the second row are difference images obtained by subtracting the equilibrium state image ($\Delta t = 0$) from the excited state images ($\Delta t > 0$). The third row of the figure schematically sketches the Vortex motion of the Landau pattern. A detailed quantitative analysis reveals that the images show a damped precessional motion of the magnetization within the magnetic domains and a damped motion of the vortex core. Other groups have investigated the magnetic switching of spin-valve samples[70–72] and the magnetization processes in a permalloy ring.[73]

Chemistry

Current research interests in SR-PEEM reflect the current interests of surface chemistry: polymers and biological materials,[5] organic electronics,[74,75] self-assembled monolayers and lithography,[76] tribology[77–79] carbon nanotubes,[80] and many more.

Fig. 8 shows an application of soft X-ray imaging of polymer blend domain structures using SR-PEEM.

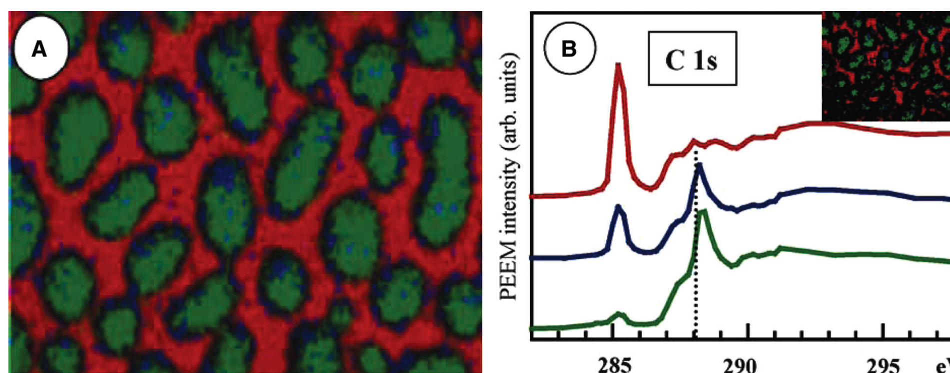

Fig. 8 A) Color coded composite map (PS: red, PMMA: green, Fg: blue) of a PS/PMMA thin film derived from a C 1s SR-PEEM image sequence, B) C 1s spectra. *Source*: Adapted from Ref.[5].

Downloaded By: [Kordesch, Martin] At: 00:51 6 January 2009

Spectroscopic features in the C1s X-ray absorption spectrum are used to image parts of a polymer blend of polystyrene and polymethylmethacrylate. The PS/PMMA form domains large enough to be resolved in SR-PEEM. The measurements first establish which image feature can be identified with which component of the polymer blend. Fibrinogen is absorbed on the polymer blend, and using the C 1s spectra, the location of the adsorbate can be plotted in maps that show the location of PS, PMMA, and the fibrinogen. Using the data ''stack,'' the material can be located spatially and analyzed spectroscopically. The use of element specific X-ray absorption features at the C 1s absorption edge shows the power of the combined SR-PEEM image and X-ray absorption spectrum.

This combination is the basis for SR-PEEM. Other applications follow the same basic method, with refinements that are based on the additional information contained in the photoelectron spectrum.

In the chemical analysis of photoelectron spectra, polarization effects are often used. Near edge X-ray absorption fine structure (NEXAFS) analysis of molecular orientation is an example of X-ray absorption spectroscopy that exploits the polarization of synchrotron light.[81]

SR-PEEM can also use polarization effects, i.e. selected features in NEXAFS spectra for imaging and contrast. The orientation of pentacene on clean gold and self-assembled monolayer (SAMs) on gold terminated with different functional groups is an example.[74] The difference in parallel (on clean gold) and perpendicular (with SAMs) orientations of the pentacene molecule could be imaged with PEEM. Ratio techniques are used to enhance the contrast and remove background.

Biological samples and polymers are sensitive to beam damage and X-ray dose, which are discussed in detail in Ref.[5] and the cited references. In some cases, the synchrotron light beam can be used to deposit materials by radiation-induced reactions. An advantage of SR-PEEM is that the deposit can also be imaged.

Patterned gold and silver surfaces using different SAMs were reported by Klauser et al.[76] using synchrotron radiation scanning photoemission microscopy, SR-SPEM. The patterns were written with SR focused with a zone-plate and observed in SR-SPEM. Spectroscopy of the deposited films showed that both decomposition/desorption of the films and cross-linking of the carbon and fluorocarbon groups occur.

While some of these examples have used well-separated and well-known X-ray absorption peaks for imaging, the application of SR-PEEM in tribology relies on more subtle spectral differences. Practical substrates used in technology are the norm, as are actual lubricants that are composed of many compounds. The tunability of SR is essential to the analysis of the image and spectral data. Here, knowledge from XPS curve fitting and the subtleties of NEXAFS are used to interpret complex spectra and images. Advances in analysis methods[77] and sample preparation[78] and techniques[79] are ongoing in this field.

Carbon nanotubes are an active field of study in chemistry, physics, and electronics. They have also been studied by SR-PEEM. Approximately 100 nanotubes were studied by Suzuki et al.,[80] and their work function determined with SR-PEEM. While it is clear that the tunability of the SR-PEEM is not a critical factor when only one element is present in the specimen, such as carbon nanotubes (C 1s), the spectroscopic analysis of the image can still be useful. The intensity of the signal, which allows energy selective imaging, is a significant feature of SR-PEEM. With the incident photon energy (350 eV) set well above the C 1s binding energy ($\sim$285 eV) the C 1s electron emission will be distributed around kinetic energies near 65 eV (350–285 eV), so that the analysis can be performed in an energy region suitable for the electron optics. A secondary electron image (KE $\sim$ 0–1 eV) is possible, and a C 1s image selecting the electron with kinetic energy at 65 eV is also possible. Depending on the resolution of the electron spectrometer, different portions of the emitted electron spectrum can be used for imaging. An energy distribution of nanotube work functions was derived from the energy resolved SR-PEEM images.

In the measurement, the C 1s binding energy for the nanotubes was determined to be 288.1 eV from the maximum intensity in the PEEM image. At a kinetic energy of 61.9 eV, a C 1s image is obtained, while at kinetic energy values near 0–1 eV, the secondary electrons emitted by the higher energy electrons can be used for imaging. By selecting the kinetic energies near the emission threshold, a determination of the work function of the nanotubes can be made. The minimum kinetic energy needed for electron emission is determined from the appearance of individual nanotubes in the image. The variations in the electronic properties of the nanotubes could be determined using a combination of SR-PEEM and photoelectron spectroscopy. Fig. 9 shows the nanotubes in LEEM, C 1s PEEM, and secondary electron PEEM.

Semiconductors and Nanostructures

In the past decade, PEEM has been successfully employed also for studies in the field of semiconductor physics. After the early work of Tonner on Si,[82] various semiconductor systems were studied by PEEM, even wide-bandgap semiconductors like GaN[83] and

Downloaded By: [Kordesch, Martin] At: 00:51 6 January 2009

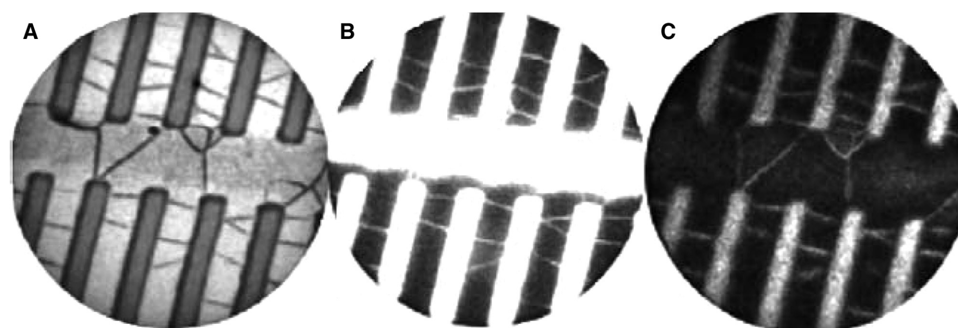

Fig. 9 A) LEEM, B) C 1s PEEM, and C) secondary electron PEEM images of SWNTs. The periodicity of the lines is 1 μm. *Source*: Adapted from Ref.[80].

magnetic semiconductors like MnAs.[84] Examples of studies of low-dimensional semiconductor systems include the observation of the quantum-size effect in two-dimensional atomically thin films,[85] while one-dimensional structures were observed after the Au-induced faceting of vicinal Si(100) surfaces.[86] Finally, zero-dimensional objects were studied for the material systems InAs/GaAs[87,88] and Ge/Si.[89] PEEM has also been employed in the study of other nano-scale island systems.[90,91] In the following, one example from the last group shall be discussed in more detail.

The realization of zero-dimensional objects in which the electrons are confined in all three dimensions, the so-called quantum dots, has attracted a lot of attention for their applications in optoelectronics.[92,93] Self-assembly of dots in semiconductor heteroepitaxy via the Stranski–Krastanov growth mode is an extremely attractive approach because it allows one to obtain a large number of homogeneous dots without slow and costly lithography steps.[94,95] The formation of islands in these systems is driven by the strain in the growing film due to the lattice mismatch between film and substrate. If the islands are sufficiently small (typical size ∼10 nm), they can confine electrons. Widely studied model systems for this approach are InAs/GaAs and Ge/Si. It was soon realized that intermixing and alloying allow for a partial strain relaxation in the growing film.[96,97] However, the confinement properties of the islands depend on their detailed chemical composition profile, i.e. their local stoichiometry. Therefore, the knowledge of this effect is of great importance for applications.

Intermixing of dots has been investigated by various techniques: Transmission electron microscopy,[98–104] scanning tunneling microscopy,[105] and X-ray diffraction.[106,107] All these measurements provide a cross-sectional profile of the dots, i.e. information in the direction normal to the sample surface. On the other hand, little is known about the lateral in-plane profile of the intermixing. This kind of information is complementary to what cross-sectional techniques can provide. Photoelectron spectroscopy can provide this information, if it is performed with sufficiently high lateral resolution to resolve individual islands.

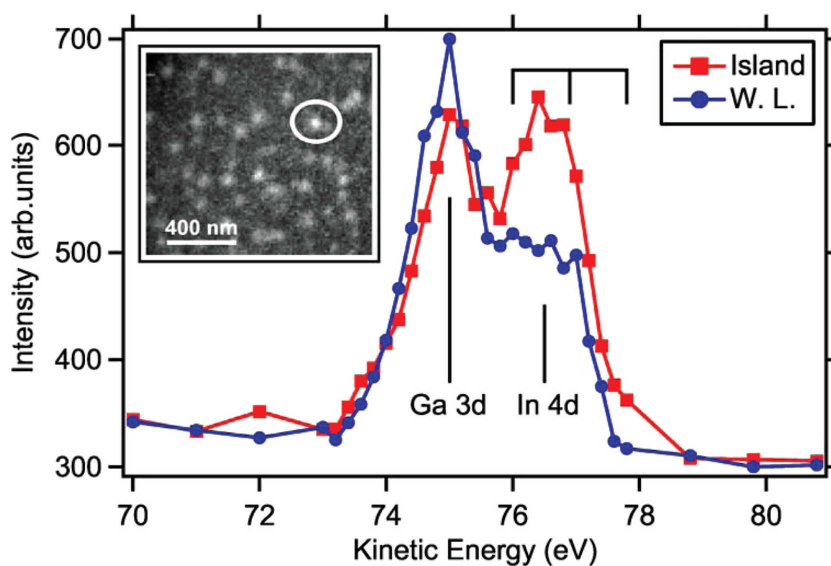

Fig. 10 Ga 3d and In 4d core level photoelectron spectra taken from an InAs/GaAs sample. The spectra were obtained from the center of the island indicated by a circle in the inset and from the wetting layer (W. L.) close to the island. Inset: SR-PEEM image of the sample surface, which was obtained with In 4d photoelectrons. The energy range used for imaging (76.9 eV ± 0.9 eV) is indicated by the horizontal bar above the In 4d core level spectrum. Photon energy 99.0 eV.

Downloaded By: [Kordesch, Martin] At: 00:51 6 January 2009

Downloaded By: [Kordesch, Martin] At: 00:51 6 January 2009

SR-PEEM with energy filter is the ideal tool for these studies.

As an example, Fig. 10 shows the Ga 3d and In 4d core level photoelectron spectra taken from an InAs/GaAs sample. The islands were grown by molecular beam epitaxy of 2.3 monolayers of InAs at 540°C on n^+-GaAs(001). Finally, an amorphous As-cap was deposited to protect the sample surface during transport in air to the beamline, where the As-cap was removed by a mild annealing to 410°C. The measurements were performed with the SPELEEM at the Nanospectroscopy Beamline at Elettra. The photon energy used was 99.0 eV.

The inset of Fig. 10 shows an SR-PEEM image of the sample surface, which was obtained with In 4d photoelectrons. The energy range used for imaging (76.9 eV $\pm$ 0.9 eV) is indicated by the horizontal bar above the In 4d core level spectrum. The spectra were obtained from the center of the island indicated by a circle in the inset and from the wetting layer close to the island. The energy resolution set for spectroscopy was approximately 1 eV. The integration area for both spectra was approximately 25 nm $\times$ 25 nm. From each spectrum, the local Ga/In concentration ratio can be deduced. Performing such an analysis pixel-by-pixel allows one to obtain a map of the Ga/In concentration ratio of the sample surface with the lateral resolution of the microscope ($\sim$25 nm).[88]

CONCLUSION

Synchrotron light sources are continuing to develop. The advances in SR light sources are also advancing the PEEM method in instrumentation, methodology, and applications. PEEM, limited in its early stages by laboratory light sources that were dim and with a narrow energy range, is now finding applications in magnetic materials, semiconductors, metrology, and spectroscopy over wide energy ranges and including the polarization available from synchrotron sources. The application of highly time-resolved PEEM to the study of the dynamics of magnetic materials may be a unique application of the PEEM method. Studies of magnetic materials alone would assure a continued use of SR-PEEM in the near future. In addition, the use of synchrotron radiation for nano-scale lithography (<50 nm) and the need for imaging such structures will ensure a continued development and application of SR-PEEM.

REFERENCES

1. Duke, P.J. *Synchrotron Radiation*; Oxford Science Publications: Oxford, 2002.
2. Attwood, D. *Soft X-rays and Extreme Ultraviolet Radiation: Principles and Applications*; Cambridge University Press: Cambridge, 1999.
3. Kordesch, M.E. Photoelectron emission electron Microscopy. In *Encyclopedia of Surface and Colloid Science* 2002.
4. Tonner, B.P.; Harp, G.R. Photoelectron microscopy with synchrotron radiation. Rev. Sci. Instrum. **1988**, *59*, 29.
5. Hitchcock, A.P.; Morin, C.; Zhang, X.; Araki, T.; Dynes, J.; Stöver, H.; Brash, J.; Lawrence, J.R.; Leppard, G.G. Soft x-ray spectromicroscopy of biological and synthetic polymer systems. J. Electron Spectrosc. Relat. Phenom. **2005**, *144–147*, 259–269.
6. Polack, F.; Lowenthal, S. Photoelectron microscope for X-ray microscopy and microanalysis. Rev. Sci. Instrum. **1981**, *52*, 207–212.
7. Beamson, G.; Porter, H.Q.; Turner, D.W. Photoelectron spectromicroscopy. Nature **1981**, *290*, 556–561.
8. Beamson, G.; Porter, H.Q.; Turner, D.W. Collimating and magnifying properties of a superconducting field photoelectron spectrometer. J. Phys. E **1980**, *13*, 64–66.
9. Cerrina, F.; Margaritondo, G.; Underwood, J.H.; Hettrick, M.; Green, M.A.; Brillson, L.J.; Francioso, A.; Hochst, H.; Delucca, P.M.; Gould, M.N. MAXIM-A scanning photoelectron microscope at ALLADIN. Nucl. Instrum. Methods Phys. Res. A **1988**, *266* (1–3), 303–307.
10. Fink, R.; Weiss, M.R.; Umbach, E.; Priekszas, D.; Rose, H.; Spehr, R.; Hartel, P.; Engel, W.; Degenhardt, R.; Wichtendahl, R.; Kuhlenbeck, H.; Erlebach, W.; Ihmann, K.; Schloegel, R.; Freund, H.-J.; Bradshaw, A.M.; Lilienkamp, G.; Schmidt, Th.; Bauer, E.; Benner, G. SMART: A planned ultrahigh-resolution spectromicroscope for BESSY II. J. Electron Spectrosc. Relat. Phenom. **1997**, *84*, 231.
11. Griffith, O.H.; Engel, W. Historical perspective and current trends in emission microscopy, mirror electron microscopy and low energy electron microscopy. Ultramicroscopy **1991**, *36*, 1–28.
12. Guenther, S.; Kaulich, B.; Gregoratti, L.; Kiskinova, M. Photoelectron microscopy and applications in surface and materials science. Prog. Surf. Sci. **2002**, *70*, 187–260.
13. Rempfer, G.F.; Griffith, O.H. The resolution of photoelectron microscopes with uv, x-ray and synchrotron excitation sources. Ultramicroscopy **1989**, *27*, 273–300.
14. Veneklasen, L.H. The continuing development of low energy electron microscopy for characterizing surfaces. Rev. Sci. Instrum. **1992**, *63*, 5513.
15. Schneider, C.M.; Schönhense, G. Investigating surface magnetism by means of photoexcitation electron emission microscopy. Rep. Prog. Phys. **2002**, *65*, R1785–R1839.
16. Buckley, C.J.; Foster, G.F.; Burge, R.E.; Ali, S.Y.; Scotchford, C.A.; Kirz, J.; Rivers, M.L. Elemental imaging of cartilage by scanning X-ray microscopy. Rev. Sci. Instrum. **1992**, *63*, 588–590.
17. Henke, B.L.; Gullikson, E.M.; Davis, J.C. X-ray interactions—Photoabsorption, scattering, transmission

Downloaded By: [Kordesch, Martin] At: 00:51 6 January 2009

and reflection at E = 50-30,000 eV, Z = 1–92. At. Data Nucl. Data Tables **1993**, *54*, 181–342.
18. Warwick, T.; Ade, H.; Hitchcock, A.P.; Padmore, H.; Rightor, E.G.; Tonner, B.P. Soft X-ray spectromicroscopy development for materials science at the advanced light source. J. Electron Spectrosc. Relat. Phenom. **1997**, *84*, 85.
19. Warwick, T.; Anders, S.; Hussain, Z.; Lamble, G.M.; Lorusso, G.F.; MacDowell, A.A.; Martin, M.C.; McHugo, S.A.; McKinney, W.R.; Padmore, H.A. Imaging spectroscopic analysis at the advanced light source. Synchrotron Radiat. News **1998**, *11* (4), 5–22.
20. Ade, H.; Kirz, J.; Hulbert, S.L.; Johnson, E.D.; Anderson, E.; Kern, D. Scanning photoelectron microscope with a zone plate generated microprobe. Appl. Phys. Lett. **1990**, *56*, 1841.
21. Kiyokura, T.; Maeda, F.; Watanabe, T.; Kadota, Y.; Iketaki, Y.; Horikawa, Y.; Oshima, M.; Shigemasa, E.; Yagishita, A. Photoelectron microspectroscopy observations of a cleaved surface of semiconductor double heterostructure. J. Vac. Sci. Technol. A **1998**, *16*, 1086–1090.
22. Cerrina, F. X-ray photo-electron spectromicroscopy. J. Electron Spectrosc. Relat. Phenom. **1995**, *76*, 9–19.
23. Guenther, S.; Kolmakov, A.; Kovac, J.; Kiskinova, M. Artefact formation in scanning photoelectron emission microscopy. Ultramicroscopy **1998**, *75*, 35.
24. Marsi, M.; Casalis, L.; Gregoratti, L.; Günther, S.; Kolmakov, A.; Kovac, J.; Lonza, D.; Kiskinova, M. ESCA microscopy at ELETTRA: What it is like to perform spectromicroscopy experiments on a third generation synchrotron radiation source. J. Electron Spectrosc. Relat. Phenom. **1997**, *84*, 73.
25. Di Fabrizio, E.; Romanato, F.; Gentili, M.; Cabrini, S.; Kaulich, B.; Susini, J.; Barrett, R. High efficiency multilevel zone plates for keV X-rays. Nature **1999**, *401*, 895.
26. Barbo, F.; Bertolo, M.; Bianco, A.; Cautero, G.; Fontana; Johal, T.K.; La Rosa, S.; Margaritondo, G.; Kaznacheyev, K. Spectromicroscopy beamline at ELETTRA: Performances achieved at the end of commissioning. Rev. Sci. Instrum. **2000**, *71*, 5.
27. Margaritondo, G.; Cerrina, F. Overview of soft X-ray photoemission spectromicroscopy. Nucl. Instrum. Meth. A **1990**, *291*, 26.
28. Voss, J. The scanning soft X-ray microscope at Hasylab: Imaging and spectroscopy of photoelectrons, photoluminescence, desorbed ions, reflected, scattered and transmitted light. J. Electron Spectrosc. Relat. Phenom. **1997**, *84*, 29.
29. Rotermund, H.H.; Engel, W.; Kordesch, M.; Ertl, G. Imaging of spatiotemporal pattern evolution during carbon-monoxide oxidation on platinum. Nature **1990**, *343*, 355–357.
30. Swiech, W.; Fecher, G.H.; Ziethen, C.; Schmidt, O.; Schönhense, G.; Grzelakowski, K.; Schneider, C.M.; Frömter, R.; Oepen, H.P.; Kirschner, J. Recent progress in photoemission microscopy with emphasis on chemical and magnetic sensitivity. J. Electron Spectrosc. Relat. Phenom. **1997**, *84*, 171.
31. Ziethen, Ch.; Schmidt, O.; Fecher, G.H.; Schneider, C.M.; Schönhense, G.; Frömter, R.; Seider, M.; Grzelakowski, K.; Merkel, M.; Funnemann, D.; Swiech, W.; Gundlach, H.; Kirschner, J. Fast elemental mapping and magnetic imaging with high lateral resolution using a novel photoemission microscope. J. Electron Spectrosc. Relat. Phenom. **1998**, 983–989.
32. Schönhense, G.; Oelsner, A.; Schmidt, O.; Fecher, G.H.; Mergel, V.; Jagutzki, O.; Schmidt-Böcking, H. Time of flight photoemission electron microscopy—A new way to chemical surface analysis. Surf. Sci. **2001**, *480*, 180–187.
33. Anders, S.; Padmore, H.A.; Scholl, A.; Scheinfein, M.R.; Stöhr, J.; Lüning, J. Investigation of magnetic materials using a new x-ray photoemission electron microscope. Synchrotron Radiat. News **1999**, *12* (3), 17–20.
34. De Stasio, G.; Perfetti, L.; Gilbert, B.; Fauchoux, O.; Capozi, M.; Perfetti, P.; Margaritondo, G.; Tonner, B.P. MEPHISTO spectromicroscope reaches 20 nm lateral resolution. Rev. Sci. Instrum. **1999**, *70*, 1740–1742.
35. Hwu, Y.; Tsai, W.L.; Lai, B.; Je, J.H.; Fecher, G.H.; Bertolo, M.; Margartitondo, G. Using photoelectron emission microscopy with hard x-rays. Surf. Sci. **2001**, *480*, 188–195.
36. Gudat, W.; Kurz, C. Close similarity between photoelectric yield and photoabsorption spectra in the soft x-ray range. Phys. Rev. Lett. **1972**, *29*, 169–172.
37. Stoehr, J.; Padmore, H.A.; Anders, S.; Stammler, T.; Scheinfein, M.R. Principles of x-ray magnetic dichroism spectromicroscopy. Surf. Rev. Lett. **1998**, *5*, 1297–1308.
38. Marx, G.K.L.; Gerheim, V.; Schönhense, G. Multipole WIEN filter for a high resolution X-PEEM. J. Electron Spectrosc. Relat. Phenom. **1997**, *84*, 251.
39. Sakai, Y.; Kato, M.; Masuda, S.; Harada, Y.; Ichinokawa, T. Development of a low energy electron microscope with an energy analyzer. Surf. Rev. Lett. **1998**, *5*, 1199–1211.
40. Kleineberg, U.; Menke, D.; Hamelmann, F.; Heinzmann, U.; Schmidt, O.; Fecher, G.H.; Schönhense, G. Photoemission microscopy with microspot-XPS by use of undulator radiation and a high-throughput multilayer monochromator at BESSY. J. Electron Spectrosc. Relat. Phenom. **1999**, 101–103, 931–936.
41. Merkel, M.; Escher, M.; Settemeyer, J.; Funnemann, D.; Oelsner, A.; Ziethen, Ch.; Schmidt, O.; Klais, M.; Schonhense, G. Microspectroscopy and spectromicroscopy with photoemission electron microscopy using a new kind of imaging energy filter. Surf. Sci. **2001**, *480*, 196.
42. Spiecker, H.; Schmidt, O.; Ziethen, Ch.; Menke, D.; Kleineberg, U.; Ahuja, R.C.; Merkel, M.; Heinzmann, U.; Schonhense, G. Time of flight photoelectron microscopy TOF-PEEM: First results. Nucl. Instr. Meth. A **1998**, *406*, 499.
43. Oelsner, A.; Schmidt, O.; Mergel, V.; Schmidt-Böcking, H.; Schönhense, G. Energy-selective imaging using delayline-detectors in TOF-XPEEM. BESSY Jahresbericht 1998.

44. Schoenhense, G.; Oelsner, A.; Schmidt, O.; Fecher, G.H.; Mergel, V.; Jagutzki, O.; Schmidt-Bocking, H. Time of flight photoemission electron microscopy—A new way to chemical surface analysis. Surf. Sci. **2001**, *480*, 180.
45. Tsuno, K. Electron optical analysis of a retarding Wien filter for electron spectroscopic imaging. Rev. Sci. Instrum. **1993**, *64*, 659.
46. Yasufuku, H.; Ohminami, Y.; Tsutsumi, T.; Niimi, H.; Matsudaira, N.; Asakura, K.; Kato, M.; Sakai, Y.; Kitajima, Y.; Iwasawa, Y. Observation of element specific energy filtered X-ray photoemission electron microscopy images of Au on Ta using a Wien filter type energy analyzer. Jpn. J. Appl. Phys. **2004**, *43*, 7682.
47. Tonner, B.P. Energy filtered imaging with electrostatic optics for photoelectron microscopy. Nucl. Instrum. Meth. A **1990**, *291*, 60.
48. Tonner, B.P.; Dunham, D.; Droubay, T.; Kikuma, J.; Denlinger, J.; Rotenberg, E.; Warwick, A. The development of electron spectromicroscopy. J. Electron Spectrosc. Relat. Phenom. **1995**, *75*, 309.
49. Veneklasen, L.H. The design of a spectroscopic low-energy electron microscope. Ultramicroscopy **1991**, *36*, 76.
50. Tonner, B.P.; Dunham, D.; Droubay, T.; Pauli, M. A photoemission microscope with a hemispherical capacitior energy filter. J. Electron Spectrosc. Relat. Phenom. **1997**, *84*, 211.
51. Heun, S.; Schmidt, Th.; Ressel, B.; Bauer, E.; Prince, K.C. Nanospectroscopy at Elettra. Synchrotron Radiat. News **1999**, *12* (5), 25–29.
52. Lilienkamp, G. New aspects in LEEM and spectroscopic emission microscopy instrumentation, EUREM 12, Brno, Czech Republic, July 9–14, 2000, p. I 177–180.
53. Engel, W.; Degenhardt, R.; Bradshaw, A.M.; Erlebach, W.; Ihmann, K.; Kuhlenbeck, H.; Wichtendahl, R.; Freund, H.-J.; Schlögl, R.; Preikzsas, D.; Rose, H.; Spehr, R.; Hartel, P.; Lilienkamp, G.; Schmidt, Th.; Bauer, E.; Benner, G.; Fink, R.; Weiss, M.R.; Umbach, E. Concept and design of the SMART spectromicroscope at BESSY II. In: Proceedings of 5th International Conference on X-ay Microscopy and Spectromicroscopy, Würzburg, Aug. 1996; Thieme, J., Schmahl, G., Rudolph, D., Umbach, E., Eds.; Springer-Verlag, Berlin-Heidelberg: New York, 1998; III-55-66.
54. Bauer, E. Low energy electron microscopy. Rep. Prog. Phys. **1994**, *57*, 895.
55. Wu, Y.K.; Robin, D.S.; Forest, E.; Schlueter, R.; Anders, S.; Feng, J.; Padmore, H.; Wei, D.H. Design and analysis of beam separator magnets for third generation aberration compensated PEEMs. Nucl. Instr. Meth. A **2004**, *519*, 230.
56. Vašina, R.; Mynář, M.; Kolařík, V. X-ray photoemission and low-energy electron microscope. In *Nanoscale Spectroscopy and Its Applications to Semiconductor Research*; Watanabe, Y., Heun, S., Salviati, G., Yamamoto, N., Eds.; Lecture Notes in Physics; Springer Verlag: Berlin, 2002; 588, 172–179.
57. Rempfer, G.F.; Desloge, D.M.; Skoczylas, W.P.; Griffith, O.H. Simultaneous correction of spherical and chromatic aberrations with an electron mirror: An electron optical achromat. Microsc. Microanal. **1997**, *3*, 14.
58. Stokstad, E. Electron microscopes—Electron mirror gives a clearer view. Science **1997**, *275*, 1069.
59. Stoehr, J.; Wu, Y.; Hermsmeier, B.D.; Samant, M.G.; Harp, G.R.; Koranda, S.; Dunham, D.; Tonner, B.P. Element specific magnetic microscopy with circularly polarized X-rays. Science **1993**, *259*, 658.
60. Freeman, M.R.; Choi, B.C. Advances in magnetic microscopy. Science **2001**, *294*, 1484.
61. Imada, S.; Suga, S.; Kuch, W.; Kirschner, J. Magnetic microspectroscopy by a combination of XMCD and PEEM. Surf. Rev. Lett. **2002**, *9*, 877.
62. Sun, H.-L.; Tohyama, T.; Okuda, T.; Harasawa, A.; Ueno, N.; Kinoshita, T. Antiferromagnetic domain modulation of NiO(100) induced by thickness-dependent interfacial coupling with Cr overlayer. J. Electron Spectrosc. Relat. Phenom. **2005**, *144–147*, 753.
63. Heitkamp, B.; Kronast, F.; Heyne, L.; Duerr, H.A.; Eberhardt, W.; Landis, S.; Rodmacq, B. Femtosecond spin dynamics of ferromagnetic thin films and nanodots probed by spin polarized photoemission electron microscopy. J. Phys. D: Appl. Phys. **2008**, *41*, 164002
64. Raabe, J.; Quitmann, C.; Ingold, G.; Johnson, S.; Buehler, C.; Back, C.H. Dynamics on nanostructured magnetic objects using x-rays: Dynamo-X, in Annual Report (Swiss Light Source, 2003).
65. Raabe, J.; Quitmann, C.; Back, C.H.; Nolting, F.; Johnson, S.; Buehler, C. Quantitative analysis of magnetic excitations in Landau flux-closure structures using synchrotron-radiation microscopy. Phys. Rev. Lett. **2005**, *94*, 217204.
66. Kubo, A.; Onda, K.; Petek, H.; Sun, Z.; Jung, Y.S.; Kim, H.K. Time-resolved magnetic domain imaging by x-ray photoemission electron microscopy. Nanoletters **2005**, *5*, 1123.
67. Choe, S.B.; Acremann, Y.; Scholl, A.; Bauer, A.; Doran, A.; Stöhr, J.; Padmore, H.A. Vortex core-driven magnetization dynamics. Science **2004**, *304*, 420.
68. Schneider, C.M.; Kuksov, A.; Krasyuk, A.; Oelsner, A.; Neeb, D.; Nepijko, S.A.; Schönhense, G.; Mönch, I.; Kaltofen, R.; Morais, J. Incoherent magnetization rotation observed in subnanosecond time-resolved x-ray photoemission electron microscopy. Appl. Phys. Lett. **2004**, *85*, 2562.
69. Krasyuk, A.; Oelsner, A.; Nepijko, S.A.; Sedov, N.N.; Kuksov, A.; Schneider, C.M.; Schönhense, G. Dynamics of magnetic stray fields at initial stage of magnetization reversal of micrometer-sized Co dots. Appl. Phys. A **2004**, *79*, 1925.
70. Vogel, J.; Kuch, W.; Camarero, J.; Fukumoto, K.; Bonfim, M.; Pennec, Y.; Pizzini, S.; Fontaine, A.; Kirschner, J. Time-resolved magnetic domain imaging by x-ray photoemission electron microscopy. Appl. Phys. Lett. **2003**, *82*, 2299–2301.
71. Vogel, J.; Kuch, W.; Camarero, J.; Fukumoto, K.; Pennec, Y.; Bonfim, M.; Pizzini, S.; Petroff, F.; Fontaine, A.; Kirschner, J. Time and layer resolved

Downloaded By: [Kordesch, Martin] At: 00:51 6 January 2009

Downloaded By: [Kordesch, Martin] At: 00:51 6 January 2009

magnetic domain imaging of FeNi/Cu/Co trilayers using x-ray photoelectron emission microscopy. J. Appl. Phys. **2004**, *95*, 6533.

72. Vogel, J.; Kuch, W.; Camarero, J.; Fukumoto, K.; Pennec, Y.; Pizzini, S.; Bonfim, M.; Petroff, F.; Fontaine, A.; Kirschner, J. Interplay between magnetic anisotropy and interlayer coupling in nanosecond magnetization reversal of spin-valve trilayers. Phys. Rev. B **2005**, *71*, 060404(R).
73. Neeb, D.; Krasyuk, A.; Oelsner, A.; Nepijko, S.A.; Elmers, H.J.; Kuksov, A.; Schneider, C.M.; Schönhense, G. Sub-nanosecond resolution x-ray magnetic circular dichroism photoemission electron microscopy of magnetization processes in a permalloy ring. J. Phys.: Condens. Matter **2005**, *17*, S1381.
74. Hsu, Y.J.; Hu, W.S.; Wei, D.H.; Wu, Y.S.; Tao, Y.T. Mapping molecular orientation of pentacene on patterned Au surface. J. Electron Spectrosc. Relat. Phenom. **2005**, *144–147*, 401–404.
75. Hu, W.S.; Tao, Y.T.; Hsu, Y.J.; Wei, D.H.; Wu, Y.S. Molecular orientation of evaporated pentacene films on gold: Alignment effect of self-assembled monolayer. Langmuir **2005**, *21*, 2260–2266.
76. Klauser, R.; Chen, C.-H.; Huang, M.-L.; Wang, S.-C.; Chuang, T.J.; Zharnikov, M. Patterning and imaging of self assembled monolayers with a focused soft X-ray beam. J. Electron Spectrosc. Relat. Phenom. **2005**, *144–147*, 393–396.
77. Pereira, G.; Lachenwitzer, A.; Nicholls, M.A.; Kasrai, M.; Norton, P.R.; DeStasio, G. Chemical characterization and nanomechanical properties of antiwear films fabricated from ZDDP on a near hypereutectic Al-Si alloy. Tribol. Lett. **2005**, *18*, 411–427 and references therein.
78. Nicholls, M.A.; Bancroft, G.M.; Kasrai, M.; Norton, P.R.; Frazer, B.H.; De Stasio, G. Improvement of PEEM images from thick inhomogeneous antiwear films using a thin Pt coating. Tribol. Lett. **2005**, *18*, 453–461.
79. Frazer, B.H.; Girasole, M.; Wiese, L.M.; Franz, T.; De Stasio, G. Spectromicroscope for the photoelectron imaging of nanostructures with x-rays (SPHINX): Performance in biology, medicine and geology. Ultramicroscopy **2004**, *99*, 87–94.
80. Suzuki, S.; Watanabe, Y.; Homma, Y.; Fukuba, S.; Locatelli, A.; Heun, S. Photoemission electron microscopy of individual single-walled carbon nanotubes. J. Electron Spectrosc. Relat. Phenom. **2005**, *144–147*, 357–360.
81. Stoehr, J. NEXAFS Spectroscopy. Springer Verlag: New York, 1992.
82. Rosenberg, R.A.; Perkins, F.K.; Mancini, D.C.; Harp, G.R.; Tonner, B.P.; Lee, S.; Dowben, P.A. Selective area deposition of boron on Si(111) induced by synchrotron radiation. Appl. Phys. Lett. **1991**, *58*, 607.
83. Yang, W.C.; Rodriguez, B.J.; Park, M.; Nemanich, R.J.; Ambacher, O.; Cimalla, V. Photoelectron emission microscopy observation of inversion domain boundaries of GaN-based lateral polarity heterostructures. J. Appl. Phys. **2003**, *94*, 5720.
84. Däweritz, L.; Herrmann, C.; Mohanty, J.; Hesjedal, T.; Ploog, K.H.; Bauer, E.; Locatelli, A.; Cherifi, S.; Belkhou, R.; Pavlovska, A.; Heun, S. Tailoring of the structural and magnetic properties of MnAs films grown on GaAs—Strain and annealing effects. J. Vac. Sci. Techol. B **2005**, *23*, 1759–1768.
85. Aballe, L.; Barinov, A.; Locatelli, A.; Heun, S.; Kiskinova, M. Tuning surface reactivity via electron quantum confinement. Phys. Rev. Lett. **2004**, *93*, 196103.
86. Meyer zu Heringdorf, F.J.; Schmidt, Th.; Heun Hild, R.; Zahl, P.; Ressel, B.; Bauer, E.; Horn-von Hoegen, M. Spatial variation of Au coverage as the driving force for nanoscopic pattern formation. Phys. Rev. Lett. **2001**, *86*, 5088–5091.
87. Heun, S.; Watanabe, Y.; Ressel, B.; Bottomley, D.; Schmidt, Th.; Prince, K.C. Core-level photoelectron spectroscopy from individual heteroepitaxial nanocrystals on GaAs(001). Phys. Rev. B **2001**, *63*, 125335.
88. Biasiol, G.; Heun, S.; Golinelli, G.B.; Locatelli, A.; Mentes, T.O.; Guo, F.Z.; Hofer, C.; Teichert, C.; Sorba, L. Surface compositional gradients of InAs/GaAs quantum dots. Appl. Phys. Lett. **2005**, *87*, 223106.
89. Ratto, F.; Rosei, F.; Locatelli, A.; Cherifi, S.; Fontana, S.; Heun, S.; Szkutnik, P.D.; Sgarlata De Crescenzi, M.; Motta, N. Composition of Ge(Si) islands in the growth of Ge on Si(111) by x-ray spectromicroscopy. J. Appl. Phys. **2005**, *97*, 043516.
90. Aggarwal, S.; Monga, A.P.; Perusse, S.R.; Ramesh, R.; Ballarotto, V.; Williams, E.D.; Chalamala, B.R.; Wei, Y.; Reuss, R.H. Spontaneous ordering of oxide nanostructures. Science **2000**, *287*, 2235.
91. Rockenberger, J.; Nolting, F.; Lüning, J.; Hu, J.; Alivisatos, A.P. Soft x-ray imaging and spectroscopy of single nanocrystals. J. Chem. Phys. **2002**, *116*, 6322.
92. Fafard, S.; Hinzer, K.; Raymond, S.; Dion, M.; McCaffrey, J.; Feng, Y.; Charbonneau, S. Red emitting semiconductor quantum dot lasers. Science **1996**, *274*, 1350
93. Yuan, Z.; Kardynal, B.E.; Stevenson, R.M.; Shields, A.J.; Lobo, C.J.; Cooper, K.; Beattie, N.S.; Ritchie, D.A.; Pepper, M. Electrically driven single photon sources. Science **2002**, *295*, 102.
94. Teichert, C. Self-organization of nanostructures in semiconductor heteroepitaxy. Phys. Rep. **2002**, *365*, 335.
95. Stangl, J.; Holy, V.; Bauer, G. Structural properties of self-organized semiconductor nanostructures. Rev. Mod. Phys. **2004**, *76*, 725.
96. Joyce, P.B.; Krzyzewski, T.J.; Bell, G.R.; Joyce, B.A.; Jones, T.S. Composition of InAs quantum dots on GaAs(001): Direct evidence for (In, Ga)As alloying. Phys. Rev. B **1998**, *58*, R15981.
97. Nakajima, K.; Konishi, A.; Kimura, K. Direct observation of intermixing at Ge/Si(001) interfaces by high-resolution Rutherford backscattering spectroscopy. Phys. Rev. Lett. **1999**, *83*, 1802.
98. Woggon, U.; Langbein, W.; Hvam, J.M.; Rosenauer, A.; Remmele, T.; Gerthsen, D. Electron microscopic and optical investigations of the indium distribution

GaAs capped InxGa1-xAs islands. Appl. Phys. Lett. **1997**, *71*, 377.
99. Rosenauer, A.; Fischer, U.; Gerthsen, D.; Förster, A. Composition evaluation of InxGa1-xAs Stranski-Krastanow-island structures by strain state analysis. Appl. Phys. Lett. **1997**, *71*, 3868.
100. Siverns, P.D.; Malik, S.; McPherson, G.; Childs, D.; Roberts, C.; Murray, R.; Joyce, B.A.; Davock, H. Scanning transmission-electron microscopy study of InAs/GaAs quantum dots. Phys. Rev. B **1998**, *58*, R10127.
101. Chaparro, S.A.; Drucker, J.; Zhang, Y.; Chandrasekhar, D.; McCartney, M.R.; Smith, D.J. Strain-driven alloying in Ge/Si(100) coherent islands. Phys. Rev. Lett. **1999**, *83*, 1199.
102. Liao, X.Z.; Zou, J.; Cockayne, D.J.H.; Leon, R.; Lobo, C. Indium segregation and enrichment in coherent InxGa1-xAs/GaAs quantum dots. Phys. Rev. Lett. **1999**, *82*, 5148.
103. Murray, R.; Malik, S.; Siverns, P.; Childs, D.; Roberts, C.; Joyce, B.; Davock, H. Scanning transmission electron microscopy (STEM) study of InAs/GaAs quantum dots. Jpn. J. Appl. Phys. **1999**, *38*, 496.
104. Rosenauer, A.; Gerthsen, D.; Van Dyck, D.; Arzberger, M.; Böhm, G.; Abstreiter, G. Quantification of segregation and mass transport in InxGa1-xAs/GaAs Stranski-Krastanow layers. Phys. Rev. B **2001**, *64*, 245334.
105. Liu, N.; Tersoff, J.; Baklenov, O.; Holmes, A.L., Jr.; Shih, C.K. Nonuniform composition profile in In0.5Ga0.5As alloy quantum dots. Phys. Rev. Lett. **2000**, *84*, 334.
106. Kegel, I.; Metzger, T.H.; Lorke, A.; Peisl, J.; Stangl, J.; Bauer, G.; Garcia, J.M.; Petroff, P.M. Nanometer-scale resolution of strain and interdiffusion in self-assembled InAs/GaAs quantum dots. Phys. Rev. Lett. **2000**, *85*, 1694.
107. Malachias, A.; Kycia, S.; Medeiros-Ribeiro, G.; Magalhaes-Paniago, R.; Kamins, T.I.; Williams, R.S. 3D composition of epitaxial nanocrystals by anomalous x-ray diffraction: Observation of a Si-rich core in Ge domes on Si(100). Phys. Rev. Lett. **2003**, *91*, 176101.

Downloaded By: [Kordesch, Martin] At: 00:51 6 January 2009